Synthesis and Characterization of Er(III) and Y(III) Sodium Silicates: $Na_3ErSi_3O_9$, a New Infrared Emitter

Duarte Ananias,[†] José P. Rainho,[†,‡] Artur Ferreira,[§] Marta Lopes,[†] Cláudia M. Morais,[†] João Rocha,*[,†] and Luís D. Carlos[‡]

Department of Chemistry, University of Aveiro, 3810−193 Aveiro, Portugal, Department of Physics, University of Aveiro, 3810-193 Aveiro, Portugal, and ESTGA, University of Aveiro, 3810-193 Aveiro, Portugal

Received October 29, 2001. Revised Manuscript Received February 12, 2002

The hydrothermal synthesis in mild conditions, and the structural characterizations and luminescence properties, of yttrium and erbium silicates $Na_3MSi_3O_9$, M = Y(III) and Er(III), has been reported. $Na_3ErSi_3O_9$ is a new infrared emitter with an emission spectrum displaying a broad visible band (300−700 nm) and a series of narrow infrared intra-$4f^{11}$ $^4I_{13/2} \rightarrow {}^4I_{15/2}$ lines. The number of Stark components detected (ca. 32) indicates the presence of four optically active environments, in accord with the structural data. When the temperature is raised from 14 to 300 K, the $^4I_{13/2} \rightarrow {}^4I_{15/2}$ transition integrated intensity increases by a factor of ca. 3.7. This remarkable and unusual behavior is the opposite temperature dependence usually observed for silicon-based materials. The samples' structures have been characterized by SEM, powder XRD, ^{29}Si MAS NMR, and ^{23}Na single- and multiple-quantum (MQ) MAS NMR. Using the recently introduced MQ MAS NMR FAM II (fast amplitude modulation of radio frequency pulses) technique, it has been possible to observe all 12 nonequivalent Na atoms in $Na_3YSi_3O_9$, even those with large quadrupole coupling constants (in excess of 4 MHz).

Introduction

The considerable progress achieved in the development of communication systems based on fiber optics has stimulated a growing interest in light sources emitting at ca. 1.54 μm.[1−3] This wavelength corresponds to the lowest attenuation and low dispersion of standard silica-based optical fibers, a highly desirable feature for signal transmission through glass fiber cables and for optical on-chip communication.[4−6] Due to its intra-$4f^{11}$ $^4I_{13/2} \rightarrow {}^4I_{15/2}$ transition, Er^{3+} is a good candidate for a temperature-stable emission at 1.54 μm.[1−6]

$Na_3YSi_3O_9$ is an important material which has been the subject of a number of ionic conductivity studies.[7,8] The photoluminescence (PL) of $Na_3YSi_3O_9$ doped with Eu(III) has also been studied.[9] Here we wish to report on the hydrothermal synthesis in mild conditions, structural characterization and luminescence properties of yttrium and erbium silicates $Na_3MSi_3O_9$, M=Y(III), Er(III). To our knowledge, the hydrothermal preparation of $Na_3ErSi_3O_9$ has not yet been reported nor have its optical properties been studied. Because our samples are microcrystalline powders, we complement the powder X-ray diffraction data with solid-state ^{29}Si and ^{23}Na NMR studies. However, Er(III) is paramagnetic, and hence, the ^{29}Si and ^{23}Na NMR spectra are poorly resolved. Thus, the NMR work has been carried out on $Na_3YSi_3O_9$. While ^{29}Si is a spin $I = {}^1/_2$ and a simple magic-angle spinning (MAS) nuclear magnetic resonance (NMR) spectrum yields highly resolved spectra, ^{23}Na is a quadrupolar $I = {}^3/_2$ nucleus giving spectral lines which are broadened by the so-called second-order quadrupole interaction. Hence, ^{23}Na MAS NMR spectra exhibit comparatively poor resolution. It is possible to obtain ^{23}Na NMR spectra free from second-order quadrupole broadening by using a two-dimensional technique known as multiple-quantum (MQ) MAS NMR spectroscopy. Here we show that $Na_3YSi_3O_9$ illustrates well the amazing resolution which may be obtained by MQ MAS NMR. Because in this material the local environment of some of the Na sites is very distorted, and thus, difficult to observe in a "conventional" MQ MAS NMR spectrum, we have used a recently introduced modification of this technique which uses fast amplitude

* To whom correspondence should be addressed. Address: Department of Chemistry, University of Aveiro, 3810-193 Aveiro, Portugal. Fax: +351 234 370084. Tel.: +351 234 370730. E-mail: ROCHA@DQ.UA.PT.
† Department of Chemistry.
‡ Department of Physics.
§ ESTGA.

(1) Przybylinska, H. H.; Jantsch, W.; Suprun-Belevitch, Y.; Stepikhova, M.; Palmetshofer, L.; Hendorfer, G.; Kozanecki, A.; Wilson, R. J.; Sealy, B. J. *Phys. Rev. B* **1996**, *54*, 2532.
(2) A. Polman, A. J. *Appl. Phys.* **1997**, *82*, 1.
(3) Minoru, F.; Yoshida, M.; Hayashi, S.; Yamamoto, K. *Appl. Phys. Lett.* **1998**, *84*, 4525.
(4) Lihui, H.; Xingren, L.; Hai, L.; Jiuling, L. *Appl. Phys. Lett.* **2000**, *77*, 2849.
(5) Wu, X.; Hömmerich, U.; Namavar, F.; Cremins-Costa, A. M. *Appl. Phys. Lett.* **1996**, *69*, 1903.
(6) Gu, G.; Ong, P. P.; Du, Y. *J. Lumin.* **1999,** *81*, 183.
(7) Kim, C. H.; Qiu, B.; Banks, E. *J. Electrochem. Soc.* **1985**, *132*, 1340.
(8) Banks, E.; Kim, C. H. *J. Electrochem. Soc.* **1985**, *132*, 2617.
(9) Kim, C. H.; Park, H. L.; Mho, S.-I. *Solid State Commun.* **1997**, *101*, 109.
(10) Goldbourg, A.; Madhu, P. K.; Vega, S. *Chem. Phys. Lett.* **2000**, *320*, 448.
(11) Maksimov, B. A.; Kalinin, V. R.; Merinov, B. V.; Ilyukhin, V. V.; Belov, N. V. *Sov. Phys. Dokl.* **1981**, *25*, 415.

10.1021/cm011550e CCC: $22.00
Published on Web 03/27/2002

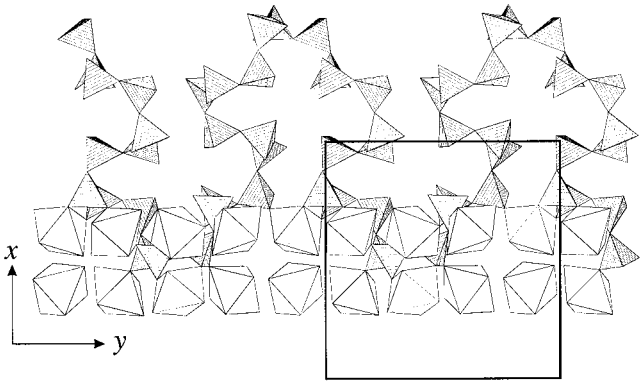

Figure 1. Structure of $Na_3MSi_3O_9$, *xy* projection, showing the relation between the infinite metachain $(Si_{24}O_{72})_\infty$ along the *b* axis and unlinked M (Y, Er) octahedral.

modulation of radio frequency pulses (FAM II), thereby ameliorating this problem.[10]

$Na_3MSi_3O_9$ materials possess a mixed (Er/Y) octahedral−(Si) tetrahedral framework (Figure 1).[11] The main features of this rather complicated crystal structure are as follows. The MO_6 octahedra are isolated from one another, while the corner sharing SiO_4 tetrahedra form an unusual type of silicon−oxygen radical, infinite in a one-dimensional spiral: a spiral metachain $(Si_{12}O_{36})_\infty$ (with period $b = 15.14$ Å) with alternate links of 12 SiO_4 tetrahedra. Since these 12 tetrahedra constitute only a half-wave, the complete wave consists of 24 tetrahedra, and thus, the formula of the chain is $(Si_{24}O_{72})_\infty$. In the links of this chain there are triortho groups (Si_3O_{10}). The terminal oxygen atoms of the adjacent triortho groups along [001] are merged yielding a new type of meta chain. There are four such chains in the unit cell. The free vertexes of the chains rest on MO_6 octahedra. In the cavities of the mixed octahedral-tetrahedral framework there are Na^+ cations.

Experimental Section

Considerable effort has been devoted to the hydrothermal synthesis of sodium rare-earth silicates (see refs 12−14 and references therein). In particular, the synthesis of $Na_3YSi_3O_9$ has been carried out at relatively high temperatures and pressures, for example, 800 °C and 3000 atm.[13] Here we propose a mild hydrothermal method for preparing $Na_3MSi_3O_9$. The main limitation of our procedure is that it is difficult to obtain the large millimeter-size crystals yielded by other methods.

Typical $Na_3ErSi_3O_9$ ($Na_3YSi_3O_9$) Synthesis. An alkaline solution was made by mixing 2.82 (2.79) g sodium silicate solution (27% m/m SiO_2, 8% m/m Na_2O, Merck), 10.54 (10.49) g H_2O, and 2.11 (2.20) g NaOH (Merck). An amount of 0.54 (0.43) g of $ErCl_3{\cdot}6H_2O$ ($Y_2(SO_4)_3{\cdot}8H_2O$) (Aldrich) was added to this solution, and the mixture was stirred thoroughly. The gel, with composition 2.37 Na_2O:1.00 SiO_2:0.056 Er_2O_3:46.1 H_2O (2.48 Na_2O:1.00 SiO_2:0.056 Y_2O_3:46.4 H_2O), was reacted in Teflon-line autoclaves (volume 45 cm^3, filling rate 0.3), under static conditions and autogenous pressure for 6 days at 230 °C. The autoclaves were then removed and quenched in cold water. The microcrystalline pink (white) powder was filtered, washed at room temperature with distilled water, and dried at 100 °C.

Materials Characterization. Powder XRD data were collected on a X'Pert MPD Philips diffractometer (Cu Kα X-radiation) with a curved graphite monochromator, a fix divergence slit of 0.5°, and a flat plate sample holder, in a Bragg−Brentano parafocusing optics configuration. Intensity data were collected by the step counting method (step 0.02° and time 8 s) in the range 2θ 7−130°. Simulations were carried out with the FullProf program.[15] Scanning electron microscope (SEM) images and energy-dispersive X-ray spectrometry (EDS) were recorded on a Hitachi S-4100 microscope. ^{23}Na and ^{29}Si NMR spectra were recorded at 105.85 and 79.49 MHz, respectively, on an Avance 400 (9.4 T, wide-bore) Bruker spectrometer. ^{29}Si MAS NMR spectra were recorded with 40° pulses, a spinning rate of 5.0 kHz and 60 s recycle delays. Chemical shifts are quoted in ppm from TMS.

The single-quantum ^{23}Na MAS NMR spectra were measured using short and powerful radio frequency pulses (0.6 μs, equivalent to a 15° pulse angle), spinning rates of 30 kHz and a recycle delay of 2 s. Chemical shifts are quoted in ppm from 1 M aqueous NaCl. The fast amplitude modulation (FAM II) triple-quantum ^{23}Na MAS NMR spectrum[10] was obtained with a spinning rate of 30 kHz and a relaxation delay of 2 s. The length of the first hard pulse (B_1=250 kHz) was 2.5 μs and the FAM II block was composed of six (X, −X, ...) pulses with lengths 1.1, 0.80, 0.45, 0.40, 0.35, and 0.15 μs. Finally, a soft pulse (B_1=15 kHz) with a length of 8.80 μs was applied. Four hundred data points (192 transients for each point) were acquired in the t_1 dimension in increments of 20 μs. The ppm scale of the sheared spectra was referenced to v_o frequency in the v_2 domain and to 3.78 v_o in the v_1 domain (ref 1 M aqueous NaCl).

Infrared emission spectra (4.2−300 K) have been obtained on a Bruker IFS 66v Fourier transform infrared spectrometer (FTIR) coupled to a Ge North-Coast EO-817 photodiode cooled to 77 K. The 488 nm line of an Ar ion-laser was used as the excitation source. The diameter of the light spot on the samples was about 2 mm. Infrared excitation spectra were recorded on a 1 m Czerny-Turner spectrometer (1000 M Spex)—fitted with a 600 grooves mm^{-1} grating blazed at 1600 nm—coupled to a Ge North-Coast EO-817 photodiode cooled to 77 K. A 300 W Xe arc lamp coupled to a 0.25 m excitation monochromator (Kratos GM-252), fitted with a 1180 grooves mm^{-1} grating blazed at 240 nm was used as excitation source. All the spectra were corrected for the response of the detectors.

Results and Discussion

$Na_3MSi_3O_9$ crystals are intertwinned into the characteristic shape shown in the SEM micrograph in Figure 2. The experimental and simulated powder XRD patterns of $Na_3ErSi_3O_9$ depicted in Figure 3 are very similar to the patterns of $Na_3YSi_3O_9$ (not shown) confirming that these materials are isomorphous. The parameters of the primitive orthorhombic unit cell (space group $P2_12_12_1$) of $Na_3ErSi_3O_9$ and $Na_3YSi_3O_9$ are, respectively, $a = 15.1913(6)$, 15.2043(4); $b = 15.1206(7)$, 15.365(5); and $c = 15.9332(6)$, 15.0426(4).

The structure of $Na_3YSi_3O_9$ calls for the presence of 12 different silicon sites with equal populations.[11] The ^{29}Si MAS NMR spectrum (Figure 4) displays nine resolved resonances and it can be deconvoluted into nine peaks with relative intensities (from high to low frequency) 1:1:1:1:2:2:2:1:1 within a 10% experimental error. Two resonances are probably overlapping in the three stronger peaks at −86.1, −87.0, and −87.4 ppm.

(12) Byrappa, K.; Yoshimura, M. *Handbook of Hydrothermal Technology*; William Andrew Publishing: Norwich, New York, 2001.
(13) Shannon, R. D.; Gier, T. E.; Foris, C. M.; Nelen, J. A.; Appleman, D. E. *Phys. Chem. Miner.* **1980**, *5*, 245.
(14) Haile, S. M.; Wuensch, B. J.; Laudise, R. A. *J. Cryst. Growth* **1993**, *131*, 373.
(15) Rodriguez-Carvajal, J.; FULLPROF, Program for Rietveld Refinement and Pattern Matching Analysis. In *Abstracts of the Satellite Meeting on Powder Diffraction of the XVth Congress of the International Union of Crystallography*, Toulouse, France, July 1990; p 127.

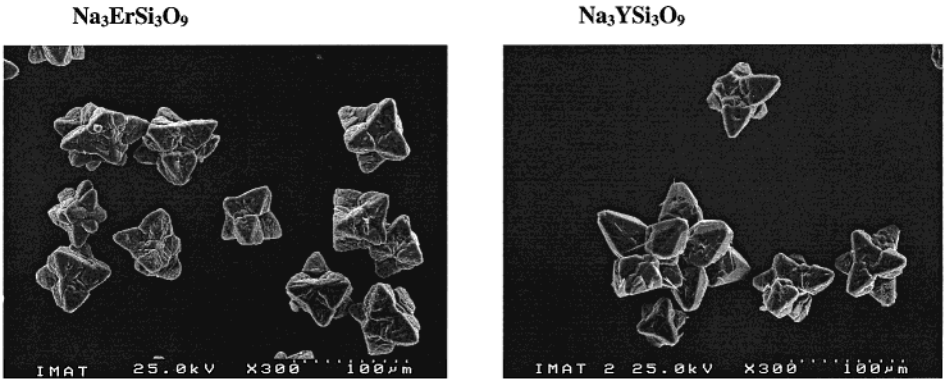

Figure 2. SEM images of $Na_3MSi_3O_9$.

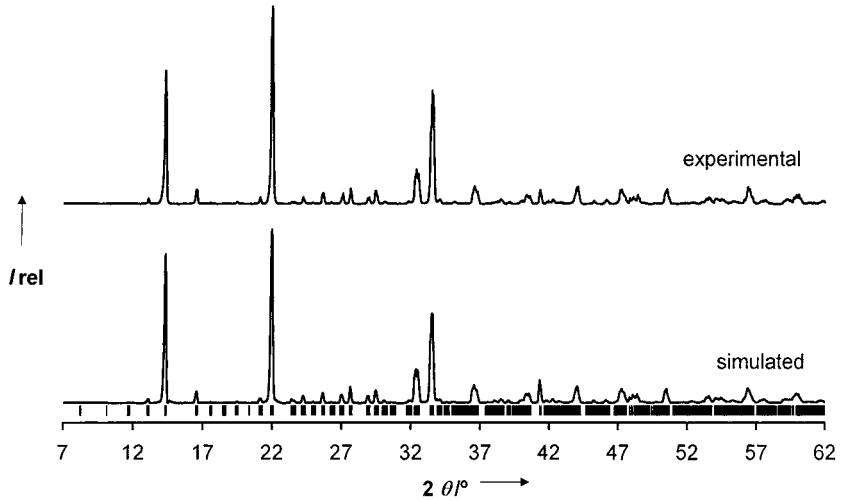

Figure 3. Experimental and simulated powder XRD pattern of $Na_3ErSi_3O_9$.

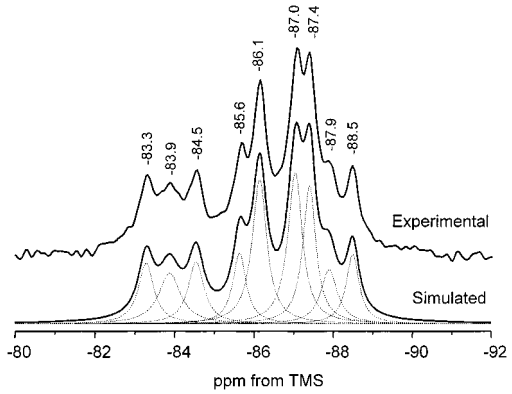

Figure 4. Experimental and simulated ^{29}Si MAS NMR spectrum of $Na_3YSi_3O_9$.

This spectrum is, thus, in accord with structure of $Na_3YSi_3O_9$. The ^{23}Na MAS NMR spectrum of $Na_3YSi_3O_9$ is poorly resolved (Figure 5a). However, the ^{23}Na FAM 3Q MAS NMR spectrum (Figure 5a) is highly resolved and all 12 resonances given by the twelve nonequivalent sodium sites in $Na_3YSi_3O_9$ are observed. We note that although peaks S1 and S2 and S3 and S4 overlap in the isotropic, F1, projection they are clearly seen in the F2 cross-sections (see, as an example, Figure 5b). Although the coordination numbers of the Na atoms are different, it is difficult to distinguish clearly pronounced polyhedra.[11] These polyhedra display a large variation of bond-lengths and bond angles. The largest spread of O−Na−O bond angles (113−116°) is found for four

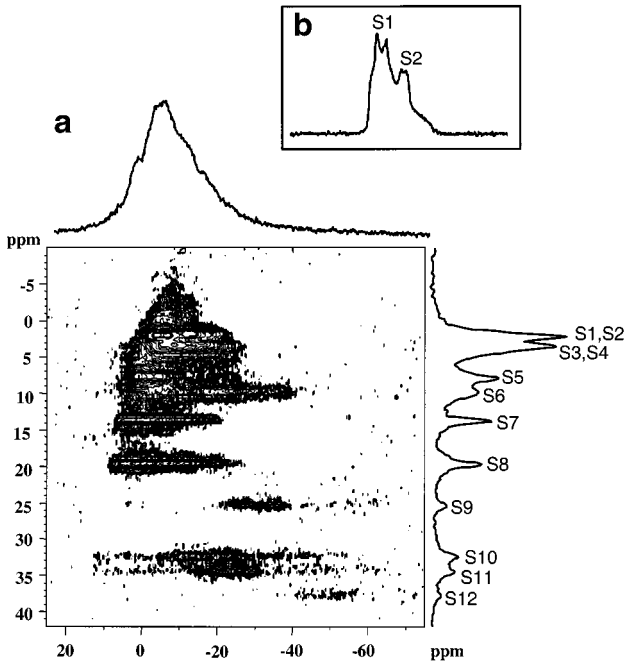

Figure 5. (a) ^{23}Na 3Q MAS NMR spectrum of $Na_3YSi_3O_9$. On top the (single-quantum) ^{23}Na MAS NMR is depicted (similar to the F2 projection of the two-dimensional spectrum). The high-resolution F1 projection represents an isotropic spectrum, free from second-order quadrupolar broadening. (b) F2 cross section taken at 2 ppm showing peaks S1 and S2 which overlap in the isotropic F1 projection.

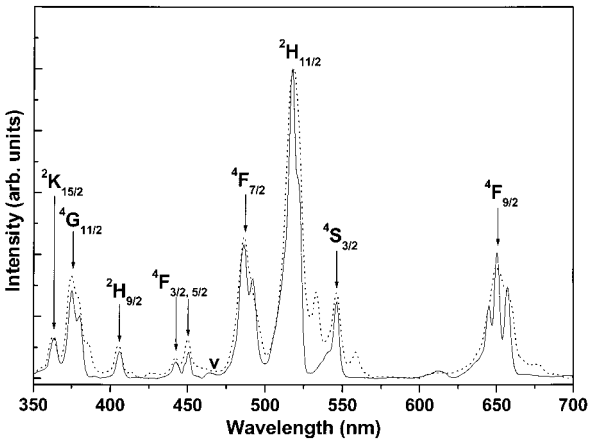

Figure 6. Excitation spectra (monitored at 1537.5 nm) of $Na_3ErSi_3O_9$ recorded at 14 (solid line) and 300 K (dotted line).

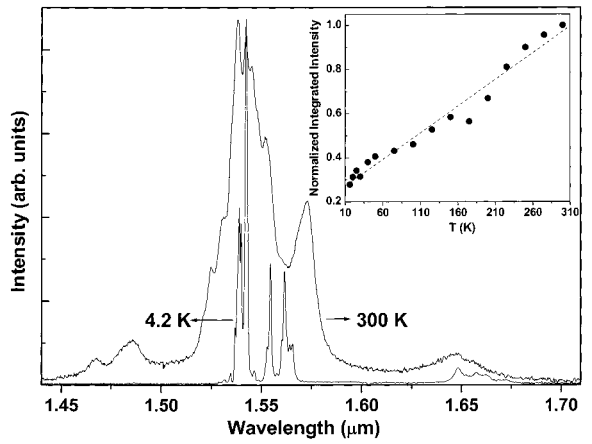

Figure 7. Infrared emission spectra of $Na_3ErSi_3O_9$ excited at 488 nm and recorded at 4.2 and 300 K. The inset shows the normalized integrated intensity of the 1.54 μm PL as a function of temperature. The excitation power is 100 mW. The dashed line is a guide for the eye.

sites: Na1, Na5, Na6, and Na8. We *tentatively* assign the four ^{23}Na 3Q MAS NMR peaks S9, S10, S11, and S12 to these four sites because it is clear from the spectrum (very wide cross sections taken through the peaks and parallel to the F2 axis) that they correspond to very distorted local Na environments (large, ca. 4 MHz, quadrupole coupling constants due to large electric field gradients at the ^{23}Na nucleus). We note in passing that peaks S9 to S12 were hardly visible in the "conventional" Z-filter MQ MAS NMR spectrum (not shown) but are clearly seen in the FAM II spectrum in Figure 5, thus showing the practical usefulness of this technique. Further using this reasoning based on bond angles, we suggest that sites Na9, Na10, and Na12 are the least distorted (largest spread of O−Na−O bond angles 76−88°) and give three of the four S1 to S4 peaks (1.4 to 2 MHz quadrupole coupling constants).

Figure 6 shows the excitation spectra (monitored at 1537.5 nm) of $Na_3ErSi_3O_9$ recorded at 14 and 300 K. The sharp lines are ascribed to intra-4f^{11} transitions between the $^4I_{15/2}$ and the $^4F_{9/2,7/2,5/2,3/2}$, $^4S_{3/2}$, $^2H_{11/2,9/2}$, $^4G_{11/2}$, and $^2K_{15/2}$ levels. The sideband observed in the high energy region of the $^4I_{15/2}\rightarrow {}^4F_{7/2}$ transition (ΔJ = 4) (marked in Figure 6) is associated with a phonon-assisted Stokes vibronic component.[16,17] The presence of this sideband violates the selection rule that arises

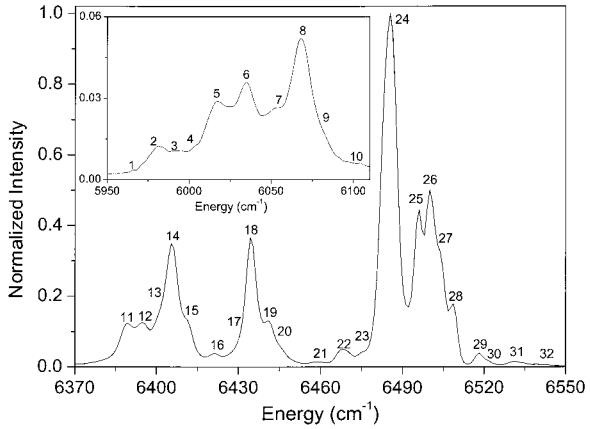

Figure 8. The local-field Stark structure of the 4 distinct Er^{3+} sites of $Na_3ErSi_3O_9$ excited at 488 nm and recorded at 4.2 K.

from theoretical approaches to vibronic line intensity on lanthanides ions.[18−21] Similar violations, generally associated with inactive infrared vibrational modes, have been observed for Pr^{3+} ($^3H_4 \rightarrow {}^3P_0$),[17] Eu^{3+} ($^7F_0 \rightarrow {}^5D_4$),[18] and Tm^{3+} ($^1D_2 \rightarrow {}^3H_6$).[20,21] The phonon energy corresponding to the observed sideband is estimated by the energy difference relative to the corresponding electronic transition. The value obtained, ca. 1041 ± 20 cm^{-1}, is associated with the Raman-active mode detected at ca. 1022 cm^{-1} (not shown) and ascribed to Si−O-M (M=Er and Y) stretch.[22] This band has been related to SiO_4 units connect to MO_6 forming O_3Si−O-M units where the Si−O bond is short and the O−M can be compared to a nonbridging bond.[22] The electron−phonon coupling parameter, g, which is a relative measure of the phonon sideband line strength, may be evaluated by calculating the intensity ratio between the vibronic and the associated electronic lines.[23−25] The value obtained, ca. 0.03, is 1 order of magnitude lower than the values reported by Soga et al.[23] and Ribeiro et al.[24] for Eu^{3+}-doped glasses but similar to the value quoted by Dejneka et al.[25] for Eu^{3+}-doped fluoride glasses.

Figure 7 shows the $Na_3ErSi_3O_9$ infrared PL spectra (excited at 488 nm) recorded at 4.2 K and room temperature. The emission lines are assigned to the intra 4f^{11} transitions between the $^4I_{13/2}$ and $^4I_{15/2}$ levels of the Er^{3+} ground multiplet. The 4.2 K infrared emission spectrum displays a $^4I_{13/2} \rightarrow {}^4I_{15/2}$ local-field structure in which 32 Stark components are clearly seen (Figure 8), supporting the presence of four optically active local Er^{3+} sites. Moreover, this number of Stark components is also in accord with the crystallographic space group $P2_12_12_1$.[1] The analyses of the curve fitting to the 4.2 K infrared emission spectrum have been carried out using Gaussian functions, and the calculated energy of the 32

(16) Auzel, F. *Phys. Rev. B* **1976**, *13*, 2809.
(17) Auzel, F.; Chen, Y. H. *J. Lumin.* **1996**, *66 & 67*, 224.
(18) Malta, O. L. *J. Phys. Chem. Solids* **1995**, *56*, 1053.
(19) Melo Donegá, C.; Meijerink, A.; Blasse, G. *J. Phys.: Condens. Matter* **1992**, *4*, 8889.
(20) Campos, A. F.; Melo Donegá, C.; Malta, O. L. *J. Lumin.* **1997**, *72−74*, 166.
(21) Campos, A. F.; Meijerink, A.; Melo Donegá, C.; Malta, O. L. *J. Phys. Chem. Solids* **2000**, *61*, 1489.
(22) Su, Y.; Balmer, M. L.; Bunker, B. C. *J. Phys. Chem. B* **2000**, *104*, 8160.
(23) Soga, K.; Inoue, H.; Makishima, A. *J. Lumin.* **1993**, *55*, 17.
(24) Ribeiro, S. J. L.; Diniz, R. E. O.; Messaddeq, Y.; Nunes, L. A.; Aegerter, M. A. *Chem. Phys. Lett.* **1994**, *220*, 214.
(25) Dejneka, M.; Snitzer, E.; Riman, R. E. *J. Lumin.* **1995**, *65*, 227.

Table 1. Fitting Energy of the 32 Stark Components for the Four Distinct Er^{3+} Sites of $Na_3ErSi_3O_9$

peak no.	energy (cm^{-1})	peak no.	energy (cm^{-1})
1	5964.0 ± 5.9	17	6430.0 ± 0.8
2	5982.3 ± 0.6	18	6434.6 ± 0.1
3	5994.5 ± 0.7	19	6440.1 ± 0.2
4	6001.6 ± 0.9	20	6444.0 ± 9.5
5	6017.8 ± 0.1	21	6459.9 ± 1.1
6	6035.0 ± 0.1	22	6468.1 ± 0.8
7	6052.3 ± 0.2	23	6476.0 ± 1.0
8	6068.3 ± 0.1	24	6485.2 ± 0.1
9	6079.7 ± 0.8	25	6496.0 ± 0.1
10	6099.2 ± 1.4	26	6500.0 ± 0.1
11	6389.8 ± 0.5	27	6503.3 ± 0.5
12	6395.2 ± 0.5	28	6508.8 ± 0.3
13	6402.0 ± 4.0	29	6518.4 ± 0.6
14	6405.9 ± 0.2	30	6521.8*
15	6410.9 ± 0.7	31	6531.6 ± 2.2
16	6421.1 ± 1.0	32	6542.0*

* See comment in text.

Stark levels is displayed in Table 1. The two energies depicted with an asterisk correspond to values inferred directly from the emission spectrum (Figure 8), since the low intensity does not allow a reasonable fitting.

When the temperature is raised from 14 to 300 K, the integrated intensity of the $^4I_{13/2} \rightarrow {}^4I_{15/2}$ transition (excited at 488 nm) increases ca. 70% (inset in Figure 7). A similar behavior is observed for other intra-$4f^{11}$ excitation wavelengths, namely, 514 nm. This temperature dependence exhibits the opposite trend usually observed in other silicon-based materials, such as Er^{3+}-doped crystalline silicon,[1,2] Er^{3+}-doped SiO_2 films containing Si nanocrystals,[3] Er^{3+}-doped porous silicon,[2,5] and $La_{0.55}Er_{0.05}Ca_{0.4}MnO_3$ perovskite manganite thin films.[6] In fact, this is a very unusual temperature dependence: to the best of our knowledge only one recent work reports a similar behavior for the 1.54 μm electroluminescence, explained in terms of Auger recombinations.[26] In Er^{3+}-doped narsarsukite samples the integrated intensity of the PL also increases with the temperature but this was related to phonon-assisted anti-Stokes excitation.[27,28] For $Na_3ErSi_3O_9$, on the contrary, excitations within the phonon-assisted Stokes vibronic sideband of the $^4I_{15/2} \rightarrow {}^4F_{7/2}$ transition, lead to a decrease of the integrated intensity of the 1.54 μm emission as the temperature increases.

The discussion of the growth of the $^4I_{13/2} \rightarrow {}^4I_{15/2}$ transition integrated intensity must consider the possible temperature dependence of the absorption cross-section (at a given wavelength). Because, in general, the absorption cross section is temperature dependent, the increment of the 1.54 μm emission between 14 and 300 K may simply be the result of a simultaneous increase of the absorption cross-section. Measuring the absorption cross section of crystalline samples is not a trivial task because it is very difficult to calculate the effective optical path. Therefore, the absorption cross section (and thus, its temperature dependence) has been estimated using the light reflected by the sample. Although these measurements do not directly yield the absorption cross section, they give values that are proportional to it. Moreover, the measurement of the integrated intensity of the light reflected by the sample allows the quantitative evaluation of any changes on the absorption cross-section induced by the temperature increase. In our experiments, the excitation wavelength has been set at 488 nm (the excitation wavelength used in the temperature dependence of the integrated intensity of the $^4I_{13/2} \rightarrow {}^4I_{15/2}$ transition, inset in Figure 7) while the emission was monitored around this wavelength (470−500 nm). All the experimental conditions, such as sample position, optics geometry, and width of the monochromator window, remained fixed between 14 and 300 K. To ensure that multiple scattering between grains does not affect the effective optical path (thus, the absorption cross-section) the crystalline powder has been submitted to high pressure (10^8 kg/m^2) to form a homogeneous pellet. The integrated intensity of the light reflected by the sample decreases ca. 10% as the temperature increases from 14 to 300 K. Therefore, the 488 nm absorption cross section increases by the same amount within that temperature range and the ca.70% variation of the $^4I_{13/2} \rightarrow {}^4I_{15/2}$ transition integrated intensity (inset in Figure 7) cannot be explained by the temperature dependence of the absorption cross section. Although the reported unusual temperature dependence is at present not well understood, issues, such as (i) the redistribution of population between the Stark levels of the fundamental multiplet as the temperature rises and (ii) the role of energy transfer between the distinct four Er^{3+} sites, are probably relevant. For example, the integrated intensity might increase with temperature due to the occurrence of Stark−Stark transitions favored by a redistribution of population between the Stark levels of the fundamental $^4I_{15/2}$ multiplet.[29] Work is in progress to address this problem.

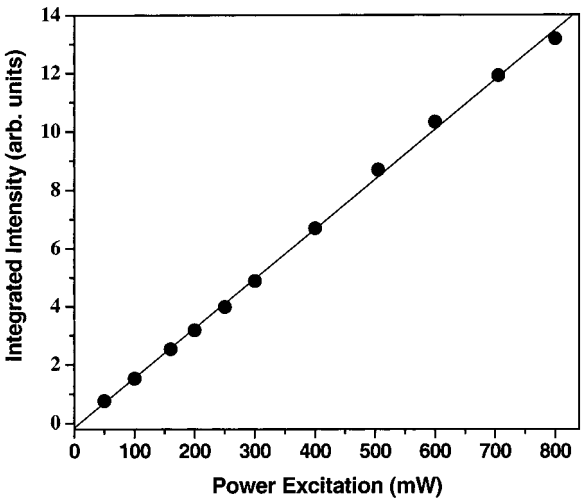

Figure 9. Integrated intensity of the 1.54 μm PL as a function of the excitation power recorded at 300 K. The full line is a linear fit to the curve ($r^2 = 0.99$).

Figure 9 displays the dependence of the PL normalized integrated intensity with the excitation power (at 300 K). The PL integrated intensity is linearly depend-

(26) Bresler, M. S.; Gusev, O. B.; Pak, P. E.; Sobolev, N. A.; Yassievich, I. N. *J. Lumin.* **1999**, *375−379*, 375.
(27) Rocha, J.; Carlos, L.D.; Rainho, J. P.; Lin, Z.; Ferreira, P.; Almeida, R. M. *J. Mater. Chem.* **2000**, *6*, 1371;
(28) Rainho, J. P.; Pillinger, M.; Carlos, L. D.; Ribeiro, S. L. J.; Almeida, R. M.; Rocha, J. *J. Mater. Chem.* in press.
(29) Malta, O. L.; Ribeiro, S. J. L.; Faucher, M.; Porcher, P. J. *J. Phys. Chem. Solids* **1991**, *52*, 587.

ent on the excitation power up to 800 mW, which corresponds to a power density of ca. 16 W/cm^2. This linearity indicates that as the excitation power rises the number of optically active Er^{3+} emitter ions increases; that is, the saturation of the Er^{3+}-related centers is not important at these power levels. Similar results (with exactly the same slope) were obtained for different temperatures, suggesting that the number of active Er^{3+} centers is temperature independent and, therefore, the increasing PL integrated intensity in $Na_3ErSi_3O_9$ as the temperature rises is not induced by an increasing number of Er^{3+} optically active centers.

After the samples have been exposed to the Ar-ion laser used for exciting the Er^{3+} emission, a broad emission band in the visible range of the electromagnetic spectra (350−750 nm) has been observed. Together with this band, a series of intra-4f^{11} sharp lines due to Er^{3+} self-absorptions (assigned to transitions between the $^4I_{15/2}$ and the $^4G_{11/2}$, $^2H_{9/2}$, $^4F_{3/2,5/2}$, $^4F_{7/2}$, $^2H_{11/2}$, $^4S_{3/2}$, and $^4F_{9/2}$ levels) were also seen (not shown). $Na_3ErSi_3O_9$ samples that have not been irradiated with the Ar-ion laser source do not display any broad visible emission. Furthermore, the energy and the relative intensity of this emission (relative to the Er^{3+} self-absorptions) depend on both the time of exposition to the Ar-ion radiation and the excitation power.

Conclusions

In summary, the hydrothermal preparation in mild conditions, the structural characterization and luminescence properties of yttrium and erbium silicates $Na_3MSi_3O_9$, M = Y(III) and Er(III), have been studied in detail. $Na_3ErSi_3O_9$ is a new infrared emitter displaying interesting and unusual optical properties. ^{23}Na MQ MAS NMR combined with fast amplitude modulation of radio frequency pulses (FAM II) has been shown to be a very powerful technique to probe the local (particularly the rather distorted) sodium environment in siliceous materials.

Acknowledgment. We thank C. de Melo Donegá (Debye Institute, University of Utrecht, The Netherlands) and O. L. Malta (Department of Fundamental Chemistry, Federal University of Pernambuco, Recife, Brazil) for the fruitful discussion concerning the temperature dependence of the PL 1.54 μm emission and Ana Cavaco (Department of Physics, University of Aveiro) for assistance in the FTIR measurements. The financial support from FCT, POCTI, PRAXIS XXI, and FEDER is gratefully acknowledged.

CM011550E